

8. Ex-vivo Characterization

8.1. Introduction

The success of transdermal drug delivery systems is when the said system can efficiently carry the drug across skin layers and make it available in high vascularized area. Further the drug can be absorbed into the systemic circulation at a rate suitable for achieving and maintaining desired therapeutic levels during the course of therapy.(1, 2) Hence, drug permeation and deposition studies are necessary for predicting in vivo behavior of newly developed formulations.

8.2. Materials and reagents

8.2.1. Materials

Thiazolyl Blue Tetrazolium Bromide (MTT) was bought from Sigma-Aldrich based in the USA. Multiple materials required for cell culturing were purchased from Himedia based at Mumbai namely, Antibiotic Antimycotic solution 100X liquid containing Penicillin (10,000 U/ml), Trypsin-EDTA solution 1X containing 0.25% trypsin, Dulbecco's Modified Eagle Medium (DMEM) containing high glucose (4.5 g/L) with L-glutamine and sodium pyruvate; Amphotericin B (25 µg/ml) in 0.9% normal saline, Streptomycin (10 mg/ml), Gamma irradiated Fetal Bovine Serum (FBS) and 0.038% EDTA in Hanks' Balanced Salt Solution with Phenol red.

8.2.2. Reagents

8.2.2.1. Phosphate buffer saline (PBS) pH 7.4

In a volumetric flask having a volume of 500 ml, 400 ml of double distilled water was transferred and then, 1.19 g of disodium hydrogen phosphate, 0.095 g of potassium dihydrogen phosphate and 4.0 g of sodium chloride were accurately weighed and added to the volumetric flask. The flask was shaken carefully to dissolve the solutes. Further, double distilled water was used to make up the volume to the mark.

8.2.2.2. Glycerol solution in PBS 7.4

Accurately weighed 15 g of glycerol was added in a 100 mL glass volumetric flask. To this volumetric flask 50 mL previously prepared PBS pH 7.4

was added and the flask was shaken vigorously to uniformly mix the contents. The final volume was made up to mark using PBS 7.4

8.2.2.3. Growth media

10 %v/v FBS and 1 %v/v antimycotic solution was added to DMEM and this was used as growth media. To prepare growth media, 10 mL of FBS and 1 ml of antimycotic solution was transferred to 89 ml DMEM. Further, the solution was mixed well. Growth media was prepared in sterile condition.

8.2.2.4. MTT solution

For the preparation of stock solution having a concentration of 5 mg/ ml, 5 mg of accurately weighed MTT was taken and solubilized in saline Phosphate Buffer having a pH of 7.4 to prepare 5 mg/mL stock. It was filtered through 0.2 μ syringe filter, collected in to a sterile, amber glass vial and preserved at -20 °C till further utilized.

8.3. Methodology

8.3.1. Skin collection and preservation

Rat skin was obtained from the Faculty of Pharmacy, The Maharaja Sayajirao University of Baroda, Gujarat, India under the IAEC (institutional animal ethics committee) protocol number MSU/IAEC/2018-19/02. Isolated rat skins were thoroughly cleaned with PBS pH 7.4, immediately rinsed and soaked in Glycerol solution in PBS 7.4 and preserved in dry ice for transportation to laboratory. In the laboratory, PBS 7.4 was used thawing rat skins at room temperature. Care was taken while separating full thickness of rat skin and was done with the help of forceps and scalpel. Fat present in the skin was cleaned and then the skin was thoroughly inspected for surface and thickness. After establishing that the skin is suitable, it was cut into pieces of circular shape having uniform thickness and a diameter suitable for fastening in franz diffusion cell. These skin pieces were soaked in 15% glycerol solution prepared in PBS 7.4, transferred to zip lock polybags and preserved in deep refrigerator at -70°C for not more than two months.(3, 4)

8.3.2. Ex-vivo permeation and deposition

MN patch of TAC/FBX, TAC/FBX cubosomes loaded microneedle, suspension of TAC/FBX and optimized cubosomes of TAC/FBX were prepared. Further these formulations were tested for deposition profile and permeation with the help of full thickness of rat skin. The evaluation was conducted by employing a Franz-type diffusion cell having a 7 ml receptor chamber for TAC. For performing this experiment, 30% ethanol solution prepared in distilled water was used for filling the receptor compartment and circular water bath was employed for maintaining its temperature at 37°C. Before initiating the permeation experiment, the skin sections were thawed at room temperature. The skin sections were kept over a soft sponge pad and 30 %v/v ethanol solution prepared in distilled water was used to impregnate the skin for a period of 30 minutes. This was done for equilibration. Further the skin sections were affixed between the receptor and donor compartment. Care was taken that the stratum corneum faces the donor compartment. Diffusion media used in the Franz diffusion cell was stirred lightly at a speed of 100 rpm. After equilibration was achieved, cubosomal dispersion of TAC and TAC suspension having 2 mg of equivalent drug was added in donor compartment. MN patch of TAC and cubosomes loaded MN patch having the identical amounts of drug were applied over the skin sections. This was done by the application of mild pressure using thumb on the skin which was kept under slight tension. Subsequently, it was affixed on place. From the sampling arm of the diffusion cell, samples having a volume of 0.5 mL were taken at various time points i.e. 0.5, 1, 1.5, 2, 3, 4, 5, 6, 7, 8, 12 and 24 hours. Further, fresh diffusion media of the same volume was replaced in order to maintain the total volume. The skin section was removed from the Franz diffusion cell after 24 hours and the skin was washed with 5 ml diffusion media three times. For calculation of the drug adhered to the skin, washings of the skin were saved. Scalpel was used for cutting the washed skin into small pieces. Then, these pieces were suspended in methanol, homogenized in cold condition for a period of 5 minutes and then it was sonicated using bath sonicator for a period of 15 minutes. For quantification of the drug accumulated in skin, the drug was removed by centrifuging it at an rpm of 5000 for a period of 10 minutes. All the samples were filtered with the help of 0.2 µm membrane filter and the quantification of the drug was performed by employing HPLC method

described earlier in chapter 3A. The cumulative quantity of drug that permeated through the skin (per cm² surface area of skin) was calculated. Finally, a graph was plotted with the concentration of cumulative amount of drug permeated per cm² surface area of skin against time. After the graph was plotted, terminal portion of the graph was used for the calculation of transdermal steady-state flux (J_{SS}; μg/cm²/h).(5, 6) Similar method was employed for the ex-vivo study of prepared formulation of FBX. However, here Franz diffusion cell having volume capacity of 20 ml was used. All formulation having 3.41 mg of FBX was evaluated during ex-vivo permeation. Equation 8.1 was used for the calculation of permeation enhancement ratio.(7)

$$PER = \frac{J_{SS}^{test}}{J_{SS}^{control}}$$

Equation: 8.1

Where J_{SS}^{test} is steady state flux via test formulation and $J_{SS}^{control}$ is steady state flux via TAC/FBX suspension.

8.3.3. Ex-vivo fluorescence microscopy

With the help of fluorescence microscopy, permeation behavior of the formulations which were developed was illustrated. FITC suspension, its MN patch, optimized cubosomes and cubosomes (FITC loaded) loaded MN patch were formulated and utilized for the study. FITC loaded cubosomes and MN patch were prepared by replacing drug for FITC in optimized compositions as described earlier in respective formulation chapters. The rat skin was thawed at room temperature, equilibrated and fastened on franz diffusion cell in the same way as explained in earlier section. FITC loaded formulations were smeared onto the stratum corneum layer of the skin in a similar way as explained in earlier sections. After a period of 12 hours, skin sectioning was performed in dark environment using cryo-microtome, sections were fixed on a glass slide. Confocal laser scanning microscope was utilized for examining the fluorescence on the slide.(8, 9)

8.3.4. In-vitro cell viability

8.3.4.1. Cell culturing and sub-culturing

A fibroblast 3T3 and RAW 264.7 Murine Macrophages cells were bought from NCCS, Pune. The received flask was kept in an anaerobic incubator for a period of 24 hours at a temperature of 37 °C and 5 % CO₂ without removing the media. Later, culture medium from the flasks was taken out and the adherent cells were washed with the help of PBS pH 7.4. Freshly prepared Trypsin-EDTA solution was then poured into the flask in order to completely cover the cell monolayer and was kept in the incubator for 2 minutes at 37 °C for detachment of adherent cells. For neutralizing trypsin's activity in the flask, fresh growth medium was poured into the flask. Further the cell culture was exposed to centrifugation set at 1200 rpm for a period of 5 minutes. Then, after discarding the supernatant, resulting cells were re-suspended in a fresh growth medium. Cells were counted using neubauer counting chamber and transferred into new flasks at a plating density of 1×10^4 cells/ cm². These flasks were kept in incubator set at a temperature of 37 °C and 5 % CO₂ to facilitate cell growth. The growth media was renewed every third day and passaging was done once the culture attained 80-90 % confluency.(10, 11)

8.3.4.2. MTT Assay

For the determination of safety, viability evaluation of fibroblast 3T3 cells was performed with the help of 3-(4, 5-dimethylthiazol-2-yl)-2, 5-diphenyltetrazolium bromide (MTT) assay [5]. Principle of this assay is based on the fact that mitochondrial dehydrogenase is responsible for the reduction of yellow-colored tetrazolium MTT whose production is found in viable (metabolically active) cells. The resultant intracellular purple formazan is solubilized and quantified with the help of spectrophotometer. Suspension of 3T3 cells in growth media was prepared from its culture using the same method as described above. 96 well plate was used for seeding of the cells (5000 cells/ well) and then it was kept in the incubator for a period of 24 hours to facilitate cell growth and its attachment to the plate surface. After 24 hours, growth media was

thrown away and 200 μ l of fresh treatment media was transferred to these wells. Then, cubosomal dispersion of TAC and TAC suspension were diluted using fresh growth medium to obtain 1000 μ g/ml of TAC solution. Similarly, cubosomal dispersion of FBX and FBX suspension were diluted in growth media to obtain 1000 μ g/ml of FBX. From, these prepared cubosomal dispersion in fresh growth medium, 100 μ l was added in different wells of 96 well plate. The plate was then incubated for 24 hours and then further, the treatment media present was discarded. 200 μ l of growth media and 100 μ l of MTT solution was transferred to each well and then further the plate was kept in the incubator for a period of 4 hours. 200 μ l of dimethyl sulfoxide was transferred to each well for solubilizing formazan crystals, after removing growth media and MTT solution carefully. 690 XR microplate reader from Bio-Rad, USA was utilized for the measurement of absorbance of the resultant solution. Measurement was performed at 570 nm. Cells viability in wells were treated with phosphate buffer saline pH 7.4, which acted as negative control was considered as 100% for the calculation of “% cell viability”. Treatment map of cubosomal dispersion for 96 well plate was described in table 8.1 for TAC cubosomes and FBX cubosomes.(12)

In a similar manner, RAW 264.7 macrophages cells were exposed to the prepared formulation to check its cytotoxic impact over RAW 264.7 cells. A cubosomal dispersion of TAC and TAC suspension were diluted similarly as described above to obtain 1000 μ g/ml of TAC. 100 μ l of the prepared diluted sample was transferred to 96 well plate. In incubation phase, 690 XR microplate reader was employed for the calculation of absorbance of the prepared formazan solution at 540 nm. Cell cytotoxicity in wells was treated with triton X considered as 100% which acted as positive control for the calculation of % cell cytotoxicity. A treatment map of cubosomal dispersion for 96 well plate was described in table 8.2 for TAC cubosomes.(13)

Table 8.1: Treatment Map of Cubosomes of TAC and FBX on 3T3 cells

	For Febuxostat					6	For Tacrolimus					
	1	2	3	4	5		7	8	9	10	11	12
A	PBS 7.4	FBX Suspen.	placebo	FBX cubo	Triton X	Blank	PBS 7.4	TAC suspen	Placebo	TAC Cubo	Triton X	Blank
B	PBS 7.4	FBX Suspen.	Placebo	FBX cubo	Triton X	Blank	PBS 7.4	TAC suspen	Placebo	TAC Cubo	Triton X	Blank
C	PBS 7.4	FBX Suspen.	Placebo	FBX cubo	Triton X	Blank	PBS 7.4	TAC suspen	Placebo	TAC Cubo	Triton X	Blank
D	PBS 7.4	FBX Suspen.	Placebo	FBX cubo	Triton X	Blank	PBS 7.4	TAC suspen	Placebo	TAC Cubo	Triton X	Blank
E	PBS 7.4	FBX Suspen.	Placebo	FBX cubo	Triton X	Blank	PBS 7.4	TAC suspen	Placebo	TAC Cubo	Triton X	Blank
F	PBS 7.4	FBX Suspen.	Placebo	FBX cubo	Triton X	Blank	PBS 7.4	TAC suspen	Placebo	TAC Cubo	Triton X	Blank
G	PBS 7.4	FBX Suspen.	Placebo	FBX cubo	Triton X	Blank	PBS 7.4	TAC suspen	Placebo	TAC Cubo	Triton X	Blank
H	PBS 7.4	FBX Suspen.	placebo	FBX cubo	Triton X	Blank	PBS 7.4	TAC suspen	Placebo	TAC Cubo	Triton X	Blank

Table represents 96 well plate

Table 8.2: Treatment Map of Cubosomes of TAC on RAW 264.7 cells

	1	2	3	4	5	6	7	8	9	10	11	12
A	PBS 7.4	TAC suspen	Placebo	TAC Cubo	Triton X	Blank						
B	PBS 7.4	TAC suspen	Placebo	TAC Cubo	Triton X	Blank						
C	PBS 7.4	TAC suspen	Placebo	TAC Cubo	Triton X	Blank						
D	PBS 7.4	TAC suspen	Placebo	TAC Cubo	Triton X	Blank						
E	PBS 7.4	TAC suspen	Placebo	TAC Cubo	Triton X	Blank						
F	PBS 7.4	TAC suspen	Placebo	TAC Cubo	Triton X	Blank						
G	PBS 7.4	TAC suspen	Placebo	TAC Cubo	Triton X	Blank						
H	PBS 7.4	TAC suspen	Placebo	TAC Cubo	Triton X	Blank						

Table represents 96 well plate

8.3.5. Histopathology

Rat abdominal skin was obtained from protocol no: MSU/IAEC/2019-20/1902. Cubosomes loaded MN patch of TAC/FBX, cubosomes of TAC/FBX and FBX/TAC drug suspension were applied on freshly excised rat abdominal skin. Apart from this, isopropyl alcohol (IPA) and PBS treated abdominal rat skin were used as positive control and negative control respectively. After four hours, Skins were immediately immersed in 10% buffered formalin, dehydrated gradually increasing concentration of ethanol, immersed in xylene and finally embedded in paraffin. The 5- μm thick sections of skin were cut from these paraffin blocks using microtome and placed on glass slides. The paraffin wax was removed by gently warming the slides and washing the molten wax with xylene. Sections were then washed with absolute alcohol and water and stained with haematoxylin and eosin to determine gross histopathology. Commercial glycerol's mounting fluid was used to finally mount the stained sections. Negative control and positive control slides were also prepared by treating rat skin with phosphate buffer solution pH 6.8 and isopropyl alcohol respectively using same method. The slides were analysed at 10-fold magnification using optical microscope.(14, 15)

8.4. Results and Discussion

8.4.1. Ex-vivo permeation and deposition of Tacrolimus (TAC)

The data obtained for TAC permeation across full thickness rat skin are summarized in Table 8.3 & 8.4. On the basis of the results of permeability from various formulations, they are organized in the order of increasing permeability: TAC Suspension < TAC MN Patch < TAC cubosomes < cubosomes of TAC loaded MNP. A slight improvement in TAC permeation was observed with MN patch of TAC (J_{ss} – 5.68 $\mu\text{g}/\text{cm}^2/\text{h}$) as compared to TAC suspension (J_{ss} – 3.04 $\mu\text{g}/\text{cm}^2/\text{h}$) due to the ability of microneedles to permeate skin barrier. However, in case of cubosomes of TAC loaded MN patch, a 7.28-fold increase in permeation (J_{ss} – 22.14 $\mu\text{g}/\text{cm}^2/\text{h}$, PER- 7.28) was observed due to microporation of skin. The results reflected that cubosomes of TAC (J_{ss} – 12.40 $\mu\text{g}/\text{cm}^2/\text{h}$) can permeate the skin barrier less significantly than cubosomes of TAC loaded MN patch. Synergistic effect of microporation on cubosome's permeability was

established as a significant enhancement was observed in the permeability through cubosomes of TAC loaded MN patch.(9, 16)

Table 8.3: Amount of TAC permeated across Rat skin

Time	Amount of drug permeated per unit area of rat skin ($\mu\text{g}/\text{cm}^2$)			
	TAC suspension	TAC cubosomes	TAC MNP	Cubosomes loaded MNP
0.5	12.17 \pm 0.47	27.39 \pm 0.90	19.03 \pm 0.33	40.05 \pm 0.59
1.0	13.41 \pm 0.96	32.29 \pm 0.21	24.86 \pm 0.25	50.82 \pm 0.58
1.5	15.29 \pm 0.08	38.70 \pm 1.27	30.27 \pm 0.23	60.90 \pm 0.91
2.0	18.03 \pm 0.32	46.98 \pm 1.53	36.99 \pm 0.26	70.22 \pm 1.87
3.0	21.06 \pm 1.18	57.07 \pm 1.91	43.01 \pm 0.29	83.41 \pm 1.69
4.0	24.11 \pm 1.79	73.97 \pm 2.50	48.35 \pm 0.32	107.06 \pm 1.87
5.0	27.22 \pm 1.35	84.19 \pm 1.58	54.52 \pm 0.32	136.63 \pm 1.82
6.0	30.78 \pm 1.28	100.43 \pm 1.98	57.58 \pm 0.23	154.37 \pm 2.90
7.0	33.82 \pm 1.84	114.40 \pm 2.51	63.46 \pm 0.41	175.38 \pm 0.97
8.0	36.50 \pm 0.48	133.54 \pm 2.64	67.70 \pm 0.63	200.65 \pm 3.10
9.0	37.26 \pm 0.26	144.27 \pm 3.00	72.49 \pm 0.55	217.65 \pm 3.61
10.0	38.37 \pm 0.14	158.27 \pm 2.71	76.49 \pm 0.38	235.64 \pm 4.26
11.0	39.93 \pm 0.22	169.22 \pm 2.00	83.52 \pm 0.73	253.11 \pm 4.56
12.0	41.88 \pm 0.65	184.50 \pm 2.87	88.27 \pm 1.00	264.50 \pm 4.34
24.0	50.37 \pm 0.46	217.46 \pm 3.33	107.47 \pm 0.89	300.73 \pm 5.79
J_{ss}	3.04	12.40	5.68	22.14
PER	1	4.08	1.87	7.28

Data was collected at 24 hours i.e. when the permeability experiment was completed for the distribution of TAC from these formulations are presented in Table 8.4. It has been noted that TAC MN patch exhibits maximum deposition of TAC. The reason for this can be due to the drug's lipophilic nature. Given to the lipophilic nature, permeation might have been complex through the dermis region which is relatively

hydrophilic. It can be concluded that permeation was better with cubosomes of TAC loaded MN patch when compared to cubosomes of TAC as the retention of TAC on skin was more in cubosomes of TAC over cubosomes of TAC loaded MN patch. Moreover, in case of drug suspension, maximum retention of drug on skin suggests that drug alone is unable to cross the skin barrier efficiently.

Table 8.4: Ex-vivo drug permeation of TAC across Rat skin

Time	% Drug permeated through rat skin			
	TAC suspension	TAC cubosomes	TAC MNP	Cubosomes loaded MNP
0.5	2.99 ± 0.06	6.72 ± 0.07	4.69 ± 0.08	9.83 ± 0.15
1.0	3.29 ± 0.08	7.93 ± 0.08	6.10 ± 0.06	12.48 ± 0.14
1.5	3.75 ± 0.05	9.50 ± 0.07	7.43 ± 0.06	14.95 ± 0.22
2.0	4.43 ± 0.07	11.53 ± 0.05	9.08 ± 0.06	17.24 ± 0.46
3.0	5.17 ± 0.03	14.01 ± 0.15	10.56 ± 0.07	20.48 ± 0.41
4.0	5.92 ± 0.08	18.16 ± 0.18	11.87 ± 0.08	26.28 ± 0.46
5.0	6.68 ± 0.09	20.67 ± 0.44	13.39 ± 0.08	33.54 ± 0.45
6.0	7.56 ± 0.04	24.66 ± 0.59	14.14 ± 0.06	37.90 ± 1.20
7.0	8.30 ± 0.05	28.09 ± 0.62	15.58 ± 0.10	43.06 ± 0.24
8.0	8.96 ± 0.12	32.78 ± 1.03	16.62 ± 0.15	49.26 ± 1.74
9.0	9.15 ± 0.06	35.42 ± 0.89	17.80 ± 0.14	53.43 ± 1.11
10.0	9.42 ± 0.03	38.82 ± 1.06	18.78 ± 0.09	57.85 ± 1.52
11.0	9.80 ± 0.06	41.54 ± 1.12	20.50 ± 0.18	62.14 ± 1.35
12.0	10.28 ± 0.16	45.29 ± 0.94	21.67 ± 0.24	64.93 ± 1.78
24.0	12.37 ± 0.11	53.39 ± 1.55	26.38 ± 0.22	73.83 ± 1.65

Table 8.5: TAC distribution profile after 24 hours of permeation study

Formulation	Drug permeated across skin (%)	Drug deposited within skin (%)	Drug retained on skin surface (%)
TAC suspension	12.37 ± 0.11	16.4 ± 0.24	70.93 ± 1.60

TAC cubosomes	53.39 ± 1.55	26.88 ± 0.68	20.07 ± 0.31
TAC MNP	26.38 ± 0.22	37.96 ± 1.06	34.21 ± 1.14
Cubosomes of TAC loaded MNP	75.83 ± 1.65	18.07 ± 0.15	7.18 ± 0.07

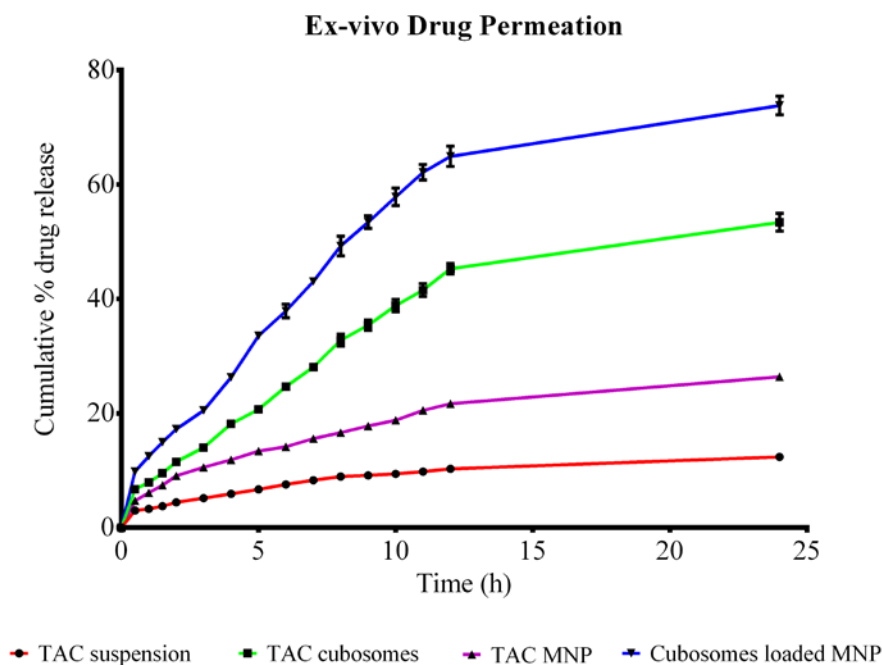


Figure 8.1: TAC drug distribution profile after 24 hours of permeation study

8.4.2. Ex-vivo permeation and deposition of Febuxostat (FBX)

Similar to TAC, experiment for analyzing the permeation of FBX across full thickness of rat skin was conducted and the collected data is captured in table 8.6 & 8.7. On the basis of the results of permeability from various formulations, they are organized in the order of increasing permeability: FBX Suspension < FBX MN Patch < FBX cubosomes < cubosomes of FBX loaded MN Patch. A slight improvement in FBX permeation was observed with MN Patch of FBX ($J_{ss} - 6.45 \mu\text{g}/\text{cm}^2/\text{h}$) as compared to FBX suspension ($J_{ss} - 4.20 \mu\text{g}/\text{cm}^2/\text{h}$) due to microneedles ability to permeate skin barrier. However, in case of cubosomes of FBX loaded MNP, an 8.34-fold increase in permeation ($J_{ss} - 35.06 \mu\text{g}/\text{cm}^2/\text{h}$, PER - 8.34) was observed due to microporation of skin. The results reflected that cubosomes of FBX ($J_{ss} - 18.43 \mu\text{g}/\text{cm}^2/\text{h}$) can permeate the skin barrier less significantly than cubosomes of FBX loaded MN Patch. Synergistic

effect of microporation on cubosome's permeability was established as a significant enhancement was observed in the permeability through cubosomes of FBX loaded MN patch.(9, 16)

Table 8.6: Amount of FBX permeated across Rat skin

Time	Amount of drug permeated per unit area of rat skin ($\mu\text{g}/\text{cm}^2$)			
	FBX suspension	FBX cubosomes	FBX MNP	Cubosomes loaded MNP
0.5	7.10 \pm 0.42	34.20 \pm 0.90	16.41 \pm 0.76	61.49 \pm 1.07
1.0	7.86 \pm 0.31	39.68 \pm 0.37	26.54 \pm 0.63	78.60 \pm 1.38
1.5	9.74 \pm 0.66	48.13 \pm 0.69	38.12 \pm 1.41	91.56 \pm 1.92
2.0	13.50 \pm 0.88	64.21 \pm 1.10	47.66 \pm 5.22	113.67 \pm 0.89
3.0	17.89 \pm 0.30	87.16 \pm 2.79	56.23 \pm 2.17	163.46 \pm 2.72
4.0	20.24 \pm 0.41	101.08 \pm 3.39	60.57 \pm 1.98	196.81 \pm 4.42
5.0	24.98 \pm 0.39	124.46 \pm 4.76	71.68 \pm 2.29	234.77 \pm 6.28
6.0	29.07 \pm 0.68	145.33 \pm 5.98	78.16 \pm 2.32	251.92 \pm 5.72
7.0	33.84 \pm 0.79	161.77 \pm 6.98	89.20 \pm 4.67	266.54 \pm 9.39
8.0	38.49 \pm 0.93	179.10 \pm 8.56	100.11 \pm 1.69	293.75 \pm 8.84
9.0	40.67 \pm 1.12	189.07 \pm 6.93	115.08 \pm 5.78	326.34 \pm 10.70
10.0	43.63 \pm 1.58	208.46 \pm 9.93	125.48 \pm 2.384	354.80 \pm 13.05
11.0	45.26 \pm 1.24	223.01 \pm 12.80	143.79 \pm 5.70	378.48 \pm 13.94
12.0	49.78 \pm 1.99	247.49 \pm 13.65	153.26 \pm 3.38	410.72 \pm 14.54
24.0	69.78 \pm 2.75	345.10 \pm 19.12	204.94 \pm 6.44	503.84 \pm 21.21
J_{ss}	4.20	18.43	6.45	35.06
PER	1	4.38	1.54	8.34

Data was collected at 24 hours i.e when the permeability experiment was completed for the distribution of FBX from these formulations are presented in Table 8.7. It has been noted that FBX MN patch exhibits maximum deposition of FBX. The reason for this can be due to the drug's lipophilic nature. Given to the lipophilic nature,

permeation might have been complex through the dermis region which is relatively hydrophilic. It can be concluded that permeation was better with cubosomes of FBX loaded MN patch when compared to cubosomes of FBX as the retention of FBX on skin was more in cubosomes of FBX over cubosomes of FBX loaded MN patch. Moreover, in case of drug suspension, maximum retention of drug on skin suggests that drug alone is unable to cross the skin barrier efficiently.

Table 8.7: Ex-vivo drug permeation of FBX across Rat skin

Time	Amount of drug permeated per unit area of rat skin ($\mu\text{g}/\text{cm}^2$)			
	FBX suspension	FBX cubosomes	FBX MNP	Cubosomes loaded MNP
0.5	1.02 ± 0.06	4.92 ± 0.13	2.36 ± 0.11	8.85 ± 0.15
1	1.13 ± 0.05	5.71 ± 0.05	3.82 ± 0.09	11.32 ± 0.2
1.5	1.4 ± 0.09	6.93 ± 0.1	5.49 ± 0.2	13.18 ± 0.28
2	1.94 ± 0.13	9.25 ± 0.16	6.86 ± 0.75	16.37 ± 0.13
3	2.58 ± 0.14	12.55 ± 0.4	8.1 ± 0.31	23.54 ± 0.39
4	2.91 ± 0.16	14.55 ± 0.49	8.72 ± 0.29	28.34 ± 0.64
5	3.6 ± 0.2	17.92 ± 0.69	10.32 ± 0.33	33.80 ± 0.90
6	4.19 ± 0.24	20.93 ± 0.86	11.25 ± 0.33	36.27 ± 0.82
7	4.87 ± 0.31	23.29 ± 1.0	12.84 ± 0.67	38.38 ± 1.35
8	5.54 ± 0.33	25.79 ± 1.23	14.41 ± 0.24	42.30 ± 1.27
9	5.86 ± 0.38	27.22 ± 1.0	16.57 ± 0.83	46.99 ± 1.54
10	6.28 ± 0.32	30.02 ± 1.43	18.07 ± 0.34	51.09 ± 1.88
11	6.52 ± 0.33	32.11 ± 1.84	20.70 ± 0.82	54.50 ± 2.01
12	7.17 ± 0.35	34.64 ± 1.97	22.07 ± 0.49	59.14 ± 2.09
24	10.05 ± 0.44	49.73 ± 2.75	29.71 ± 1.31	72.55 ± 3.05

Table 8.8: FBX distribution profile after 24 hours of permeation study

Formulation	Drug permeated across skin (%)	Drug deposited within skin (%)	Drug retained on skin surface (%)
FBX suspension	10.05 ± 0.44	15.94 ± 0.25	72.36 ± 2.28

FBX cubosomes	49.73 ± 2.75	19.09 ± 0.18	31.07 ± 1.37
FBX MNP	29.71 ± 29.71	38.96 ± 1.95	29.90 ± 0.59
Cubosomes of FBX loaded MNP	72.55 ± 3.05	13.29 ± 0.09	11.94 ± 0.05

Ex-vivo Drug Permeation

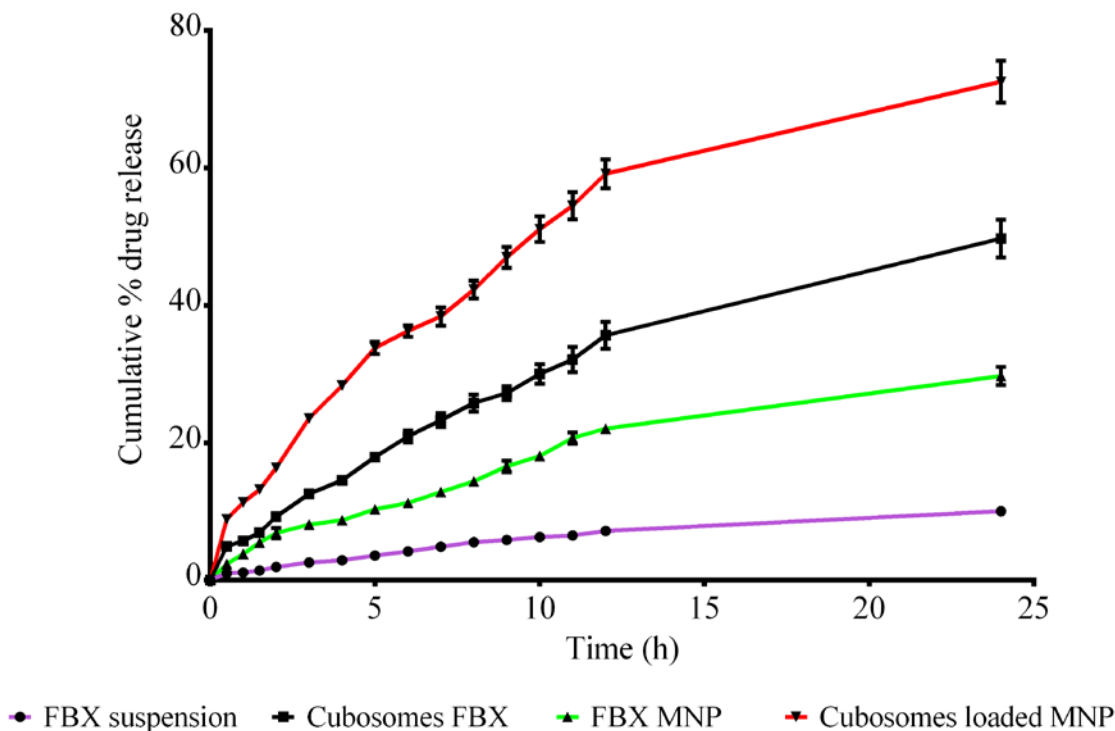


Figure 8.2: FBX drug distribution profile after 24 hours of permeation study

8.4.3. Ex-vivo fluorescence microscopy

Sections of the rat skin were taken and exposed to FITC loaded formulations for a period of 12 hours. Further, after exposure fluorescence microscopic images of rat skin sections was taken and the images are presented in Fig. 8.3. It is noted that the sections of skin exposed to FITC suspension has least fluorescence. Based on the results formulations are organized in increasing order of the fluorescence: FITC Suspension < FITC MN Patch < FITC cubosomes < MN Patch loaded with cubosomes of FITC.

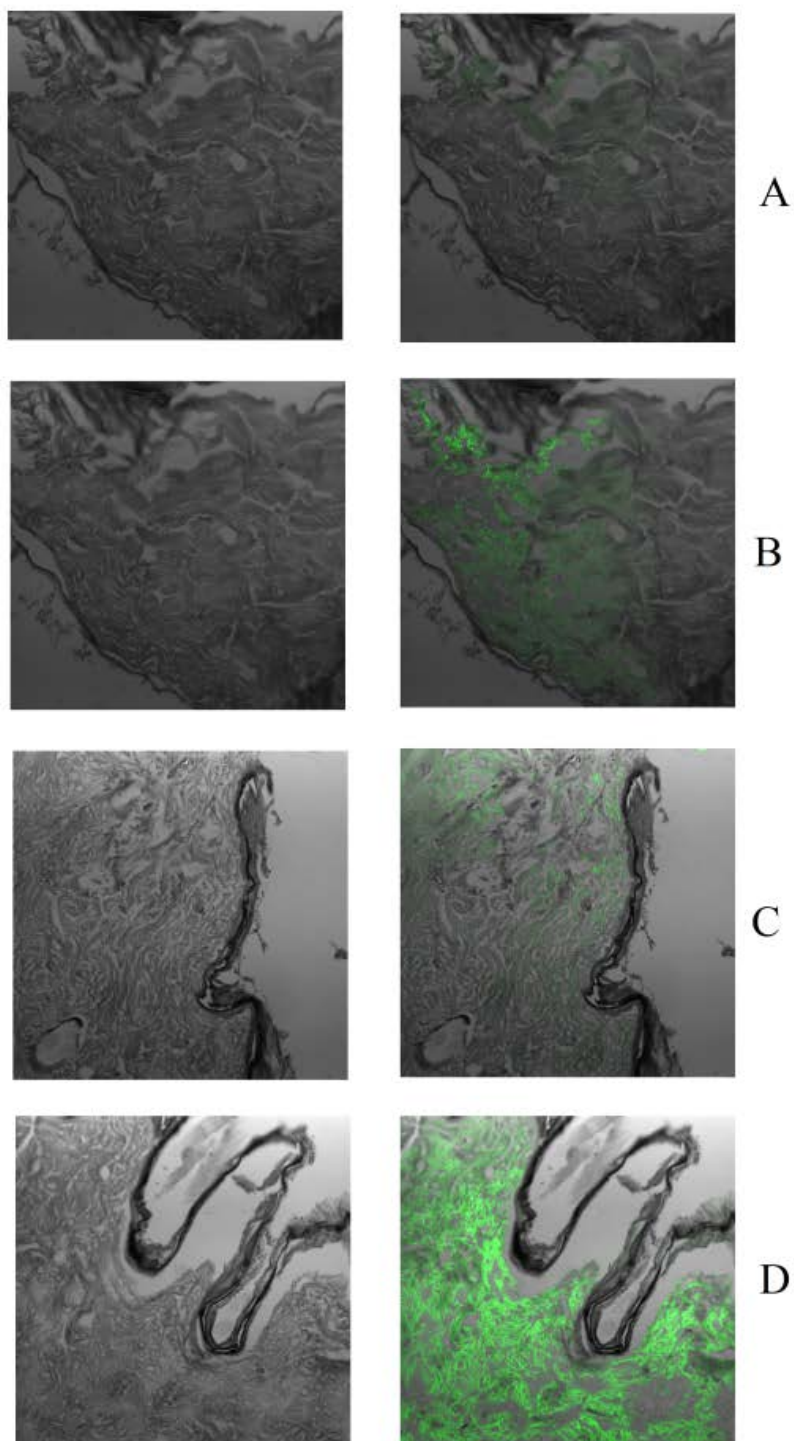


Figure 8.3: Fluorescence microscopic images of rat skin sections after 12h of treatment with A) FITC suspension, B) cubosomes loaded with FITC, C) MN patch of FITC, D) MN patch loaded with FITC cubosomes

It was noted that the data collected from the fluorescence microscope experiment, complied with the ex vivo permeation and deposition data wherein maximum fluorescence was reported in section of skin which was exposed to the MN Patch loaded with FITC cubosomes. Therefore, it can be concluded that there is enhanced permeation through developed nanocarriers loaded fast dissolving microneedle patches.(9)

8.4.4. In-vitro cell viability

Cell viability data for TAC formulations are summarized in Table 8.9 and graphically illustrated in Fig. 8.4.

Table 8.9: In vitro cell viability data for cubosomes of TAC in 3T3 cells

Treatments	Absorbance	% Cell Viability
Negative control- PBS 7.4	0.236 ± 0.025	100.00
TAC suspension	0.145 ± 0.008	61.44 ± 3.59
Placebo	0.242 ± 0.034	102.40 ± 11.67
Cubosomes of TAC	0.248 ± 0.034	105.37 ± 16.78
Positive control- Triton X	0.01 ± 0.006	4.38 ± 2.88

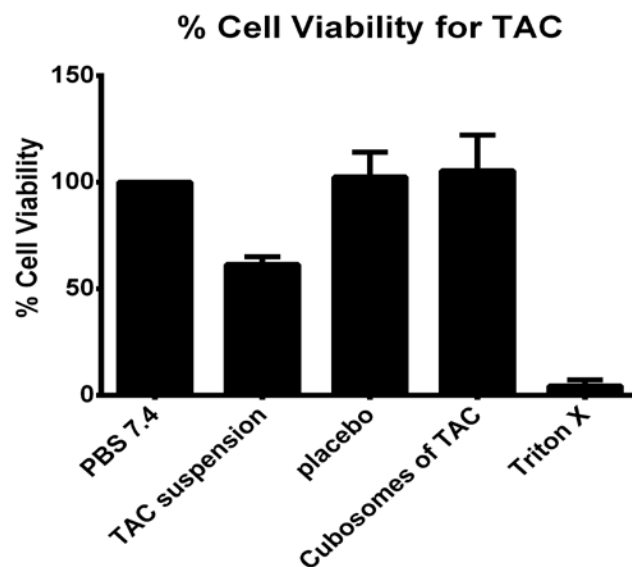


Figure 8.4: % viability of fibroblast 3T3 cells after treatment with cubosomes of Tacrolimus

The legitimacy of positive control was established given to the significantly lower viability of cells which were exposed to Triton X 100 (4.38 ± 2.88 %). The viability of cells treated with TAC loaded cubosomes (105.37 % \pm 16.78) was found significantly higher than positive control and near to negative control. This indicated a less toxic nature of developed formulations.

The cell viability data for FBX formulations are summarized in Table 8.10 and graphically illustrated in Fig. 8.5.

Table 8.10: In vitro cell viability data for cubosomes of FBX in 3T3 cells

Treatments	Absorbance	% Cell Viability
Negative control- PBS 7.4	0.379 ± 0.014	100.00
FBX suspension	0.255 ± 0.040	67.48 ± 12.36
Placebo	0.345 ± 0.051	91.25 ± 14.6
Cubosomes of FBX	0.342 ± 0.030	90.32 ± 9.93
Positive control- Triton X	0.026 ± 0.013	6.82 ± 3.65

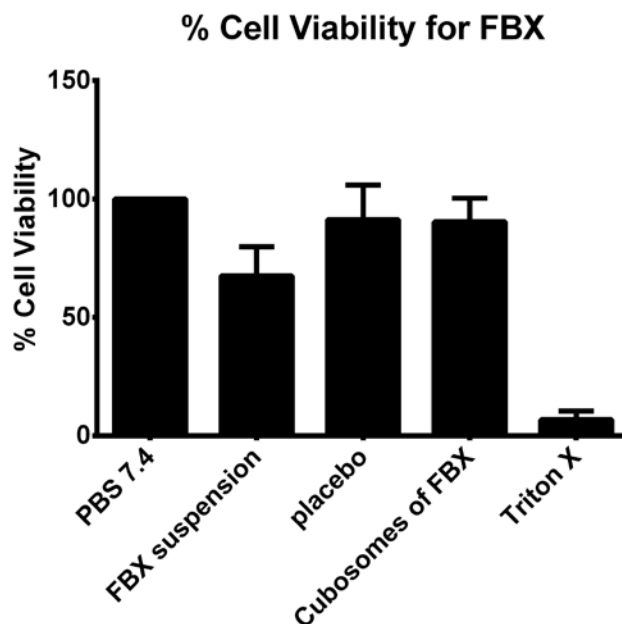


Figure 8.5: % viability of fibroblast 3T3 cells after treatment with cubosomes of Febuxostat

A significantly lower viability of cells treated with Triton X 100 (6.82 ± 3.65 %) indicated validity of the positive control. The viability of cells treated with FBX loaded cubosomes (90.32 ± 9.93 %) was found significantly higher than positive control and near to negative control. This indicated a less toxic nature of developed formulations.

The cell cytotoxicity data for TAC formulations are summarized in Table 8.11 and graphically illustrated in Fig. 8.6.

Table 8.11: In vitro cell cytotoxicity data for cubosomes of TAC in RAW 264.7 cells

Treatments	Absorbance	% Cell cytotoxicity
Negative control- PBS 7.4	0.296 ± 0.042	00.00
TAC suspension	0.193 ± 0.034	32.71 ± 20.24
Placebo	0.254 ± 0.047	14.33 ± 3.67
Cubosomes of TAC	0.175 ± 0.037	39.82 ± 16.03
Positive control- Triton X	0.03 ± 0.015	89.48 ± 6.29

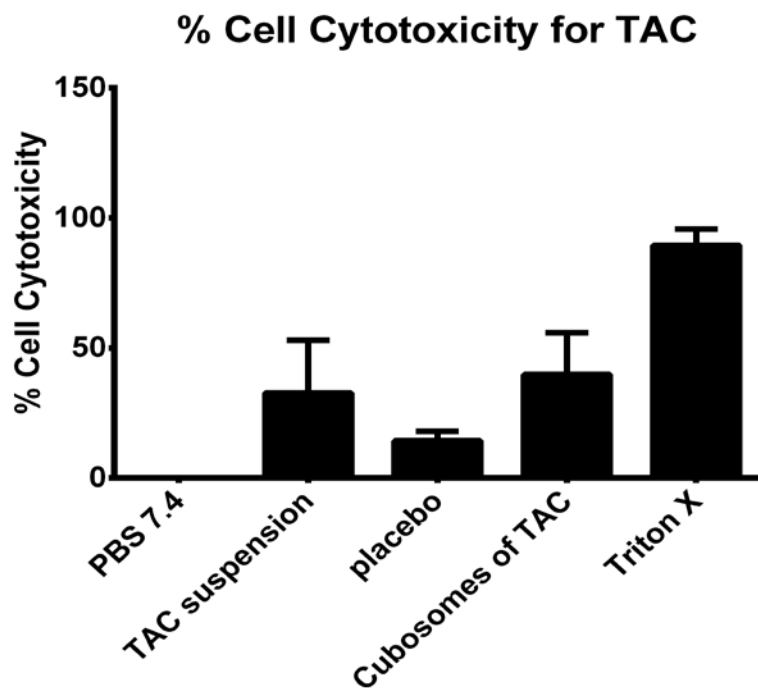


Figure 8.6: % viability of macrophage RAW 264.7 cells after treatment with cubosomes of Tacrolimus

From the data collected for % cytotoxicity of TAC on RAW 264.7 cells, it can be concluded that Triton X 100 has the highest cytotoxic effect on RAW 264.7 cell i.e. 89.48 ± 6.29 %. The viability of cells treated with TAC loaded cubosomes (90.32 ± 9.93 %) was found significantly higher than positive control and near to negative control. This indicated a less toxic nature of developed formulations.

8.4.5. Histopathology

The haematoxylin and eosin stained sections of rat abdominal skins treated with developed cubosomes of TAC/FBX and cubosomes loaded MN patch of TAC/FBX were examined under microscope for any pathological changes and compared with negative control (PBS 7.4) and positive control (IPA) to study the safety aspect of using microneedle patch. The microscopic images have been shown in Fig 7.4. The sections of skins treated with developed cubosomes of TAC/FBX and cubosomes loaded MN patch of TAC/FBX showed almost similar cellular integrity as compared to skin treated with phosphate buffer saline (pH 7.4) as negative control with no sign of inflammation. The section of skin treated with isopropyl alcohol as positive control showed considerable damage to skin layers as an indication of irritation and toxicity. Figure 7.4 clearly shows microporation on skin surface due to the cubosomes loaded MN patch of TAC/FBX.

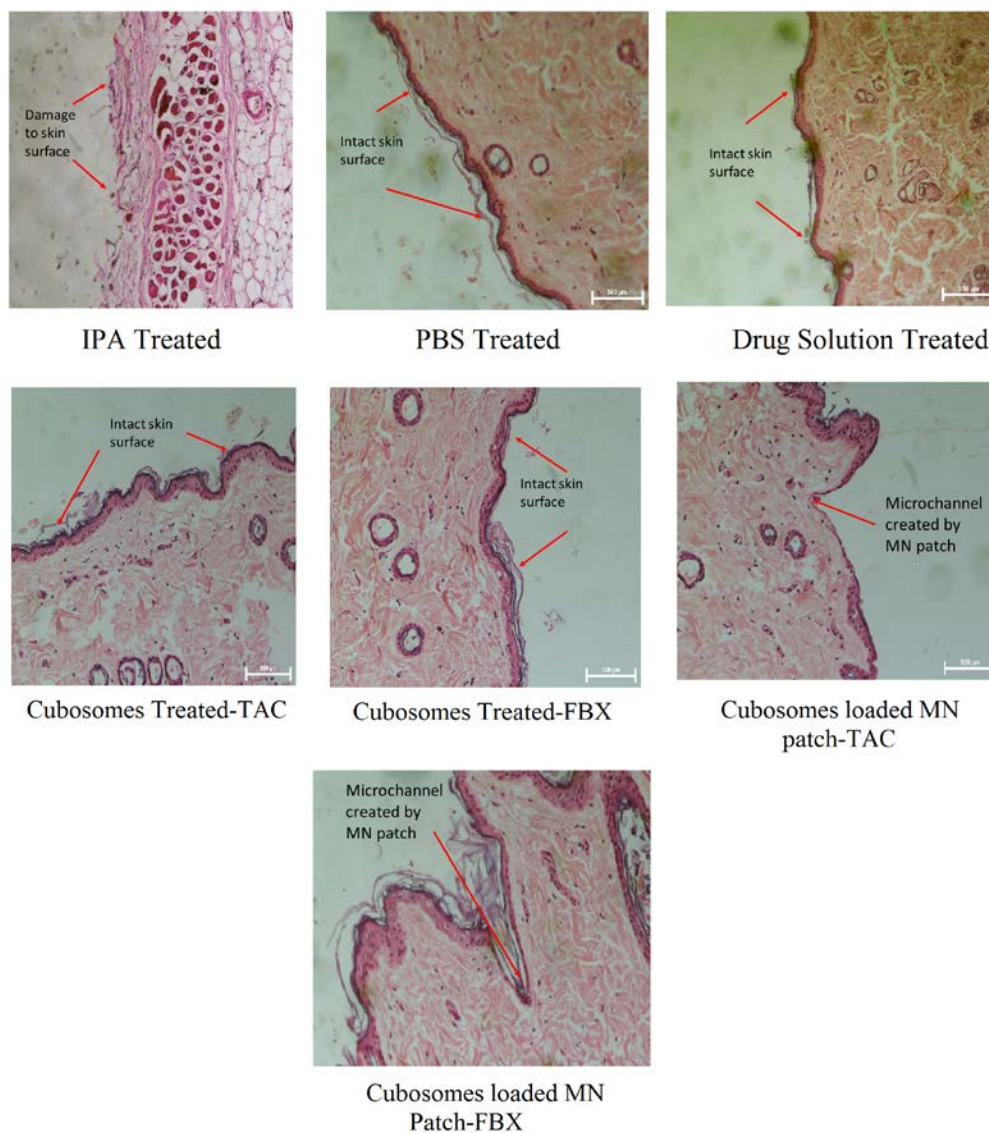


Figure 8.7: Histopathology study of developed formulation

8.5. References

1. Guillot AJ, Cordeiro AS, Donnelly RF, Montesinos MC, Garrigues TM, Melero A. Microneedle-based delivery: An overview of current applications and trends. *Pharmaceutics*. 2020;12(6):569.
2. Prausnitz MR, Langer R. Transdermal drug delivery. *Nature biotechnology*. 2008;26(11):1261-8.

3. Babu R, Kanikkannan N, Kikwai L, Ortega C, Andega S, Ball K, et al. The influence of various methods of cold storage of skin on the permeation of melatonin and nimesulide. *Journal of controlled release*. 2003;86(1):49-57.
4. De A, Mathur M, Gore M. Viability of cadaver skin grafts stored in skin bank at two different temperatures. *Indian Journal of Medical Research*. 2008;128(6):769-72.
5. Indermun S, Choonara YE, Kumar P, du Toit LC, Modi G, van Vuuren S, et al. Ex vivo evaluation of a microneedle array device for transdermal application. *International journal of pharmaceutics*. 2015;496(2):351-9.
6. Salah S, Mahmoud AA, Kamel AO. Etodolac transdermal cubosomes for the treatment of rheumatoid arthritis: ex vivo permeation and in vivo pharmacokinetic studies. *Drug delivery*. 2017;24(1):846-56.
7. Li Y, Wang C, Wang J, Chu T, Zhao L, Zhao L. Permeation-enhancing effects and mechanisms of O-acylterpineol on isosorbide dinitrate: mechanistic insights based on ATR-FTIR spectroscopy, molecular modeling, and CLSM images. *Drug delivery*. 2019;26(1):107-19.
8. Chen C-H, Shyu VB-H, Chen C-T. Dissolving microneedle patches for transdermal insulin delivery in diabetic mice: potential for clinical applications. *Materials*. 2018;11(9):1625.
9. Srivastava PK, Thakkar HP. Vinpocetine loaded ultradeformable liposomes as fast dissolving microneedle patch: Tackling treatment challenges of dementia. *European Journal of Pharmaceutics and Biopharmaceutics*. 2020;156:176-90.
10. Segeritz C-P, Vallier L. Cell culture: growing cells as model systems in vitro. *Basic Science Methods for Clinical Researchers*: Elsevier; 2017. p. 151-72.
11. Helgason CD, Miller CL. *Basic cell culture protocols*: Totowa, NJ.: Humana Press; 2005.

12. Basak V, Bahar TE, Emine K, Yelda K, Mine K, Figen S, et al. Evaluation of cytotoxicity and gelatinases activity in 3T3 fibroblast cell by root repair materials. *Biotechnology & Biotechnological Equipment*. 2016;30(5):984-90.
13. Lee JY, Park W. Anti-inflammatory effects of oroxylin A on RAW 264.7 mouse macrophages induced with polyinosinic-polycytidylic acid. *Experimental and therapeutic medicine*. 2016;12(1):151-6.
14. P Thakkar H, Savsani H, Kumar P. Ethosomal hydrogel of raloxifene HCl: statistical optimization & ex vivo permeability evaluation across microporated Pig ear skin. *Current drug delivery*. 2016;13(7):1111-22.
15. Slaoui M, Fiette L. Histopathology procedures: from tissue sampling to histopathological evaluation. *Drug safety evaluation: Springer*; 2011. p. 69-82.
16. Qiu Y, Gao Y, Hu K, Li F. Enhancement of skin permeation of docetaxel: a novel approach combining microneedle and elastic liposomes. *Journal of Controlled Release*. 2008;129(2):144-50.